Parkinsonism and Related Disorders 64 (2019) 97–105

Contents lists available at ScienceDirect

Parkinsonism and Related Disorders

journal homepage: www.elsevier.com/locate/parkreldis

Cerebral glucose metabolism in idiopathic REM sleep behavior disorder is different from tau-related and α-synuclein-related neurodegenerative disorders: A brain [18F]FDG PET study

Claudio Liguori[a,*], Roberta Ruffini[a], Enrica Olivola[b], Agostino Chiaravalloti[b,c], Francesca Izzi[a], Alessandro Stefani[d], Mariangela Pierantozzi[e], Nicola Biagio Mercuri[e,f], Nicola Modugno[b], Diego Centonze[b,e], Orazio Schillaci[b,c], Fabio Placidi[a]

[a] Sleep Medicine Centre, Department of Systems Medicine, University of Rome 'Tor Vergata", Rome, Italy
[b] IRCSS Neuromed, Pozzilli, Italy
[c] Department of Biomedicine and Prevention, University of Rome 'Tor Vergata', Rome, Italy
[d] Parkinson's Disease Centre, Neurology Unit, Department of Systems Medicine, University of Rome "Tor Vergata", Rome, Italy
[e] Neurology Unit, Department of Systems Medicine, University of Rome "Tor Vergata", Rome, Italy
[f] IRCCS Fondazione Santa Lucia, Rome, Italy

ARTICLE INFO

Keywords:
Idiopathic RBD
Parkinson's disease
Alzheimer's disease
Lewy body dementia
[18F]FDG PET
Neurodegeneration
Cerebral glucose metabolism

ABSTRACT

Introduction: Several longitudinal studies revealed that patients affected by idiopathic REM behavior disorder (iRBD) trend to convert to α-synucleinopathies at follow-up, although the time and direction of conversion is currently unpredictable. This study aimed at evaluating brain glucose metabolism, measured by [18F]FDG-PET, in patients affected by iRBD and compared to Parkinson's Disease (PD), Lewy Body Dementia (DLB), Alzheimer's Disease (AD), and controls.

Methods: Differences in brain [18F]FDG uptake were analyzed using statistical parametric mapping implemented in Matlab R2012b among iRBD, PD, DLB, AD, and controls.

Results: Fifty-four iRBD, 28 PD, 10 DLB, 55 AD, and 35 controls were included in this study. iRBD patients presented an altered [18F]FDG uptake, since the increased [18F]FDG uptake in the brainstem and the reduced [18F]FDG uptake in temporal and parietal regions compared to controls. Moreover, iRBD patients showed several differences in [18F]FDG uptake than PD, DLB, or AD groups, with the main differences documented in the comparison with AD patients.

Conclusions: This study documented the alteration of brain [18F]FDG uptake in brainstem and cortical areas of iRBD patients compared to controls. Moreover, the cerebral [18F]FDG uptake of iRBD patients resulted different from that presented by AD, further supporting the hypothesis that tau-related neurodegeneration may not induce RBD manifestations. However, brain [18F]FDG uptake of iRBD patients also differed from that of DLB and PD patients. Hence, these findings further support the hypothesis that iRBD may represent a very early stage of α-synucleinopathy in which biomarkers changes already occur but not allow the prediction of phenoconversion.

1. Introduction

Rapid Eye Movement (REM) Behaviour Disorder (RBD) is a sleep parasomnia characterized by the pathological lack of atonia during REM sleep (REM sleep without atonia) associated with abnormal and vigorous nocturnal complex motor behaviours and vocalizations (dreams' enactment) [1]. RBD may be associated with other sleep disorders (i.e. narcolepsy) [2], with a wide range of neurodegenerative disorders (i.e. α-synucleinopathies) [2], and as iatrogenic consequence of psychiatric treatments (i.e. antidepressants, beta-blockers) [3]. When RBD is associated with neurological disorders, it is classified as secondary. In 60% of cases no triggering causes or other neurological disorders are identified and RBD is defined as idiopathic (iRDB), although this differentiation is actually under debate [4]. Longitudinal studies (with 16 years follow-up) revealed that up to 81% of iRBD patients convert to α-synucleinopathies such as Parkinson's Disease (PD), Lewy Body Dementia (DLB) and multiple system atrophy (MSA) [5], which are neurodegenerative disorders characterized by neuronal

* Corresponding author. Sleep Medicine Centre, Department of Systems Medicine, University of Rome "Tor Vergata", Viale Oxford 81, 00133, Rome, Italy.
E-mail address: liguori@med.uniroma2.it (C. Liguori).

https://doi.org/10.1016/j.parkreldis.2019.03.017
Received 10 September 2018; Received in revised form 16 March 2019; Accepted 19 March 2019

Table 1
Demographic and clinical characteristics of patients and controls.

	iRBD (n = 54) mean ± SD	PD (n = 28) mean ± SD	DLB (n = 10) mean ± SD	AD (n = 55) mean ± SD	Controls (n = 35) mean ± SD
Age	69.75 ± 8.89	65.6 ± 7.56	69.02 ± 7.71	69.18 ± 4.30	67.89 ± 4.95
Gender	41 M; 13F	15 M; 13F	8 M; 2F	24 M; 31F	19 M; 16F
Disease Duration (years)	5.75 ± 2.57	1.75 ± 3.14	2.15 ± 1.26	2.77 ± 1.85	NA
MMSE	27.64 ± 2.06	26.30 ± 4.22	23.6 ± 5.20	21.44 ± 3.82	29.40 ± 1.22
UPDRS-III	3.45 ± 3.78	16.90 ± 8.50	15.01 ± 6.45	NA	NA

Abbreviations: iRBD, idiopathic RBD; RBD, REM sleep behavior disorder; PD, Parkinson's Disease; DLB, Lewy Body Dementia; AD, Alzheimer's Disease; SD, standard deviation; M, male; F, female; NA, not admitted.

loss due to the accumulation of α-synuclein deposits, named Lewy bodies (LB) [6]. Hence, iRBD may represent the prodromal manifestation of these neurodegenerative α-synucleinopathies. However, some longitudinal studies reported that a small group of patients can develop either overlapping form of dementia or AD [7].

[18F]-Fluorodeoxyglucose positron emission tomography ([18F]FDG PET) is currently the most accurate in-vivo method for the investigation of regional human brain metabolism in health and disease states [8]. It measures cerebral glucose metabolism, which can be understood as a proxy of synaptic function [8]. Since [18F]FDG PET can be considered as a downstream topographical marker of a neurodegenerative disease, it can provide helpful diagnostic information and complement findings of other neuroimaging techniques and can be used to monitor disease severity or progression [9]. As documented in cross-sectional studies, [18F]FDG PET can detect abnormal functional brain alterations in iRBD patients [10,11], which are predictive of phenoconversion and evolution toward the onset of α-synucleinopathies [12]. Accordingly, patients with RBD who phenoconvert to PD or DLB may already have functional cerebral abnormalities at baseline [12].

Therefore, iRBD may represent a prodromal manifestation of different neurological disorders such as PD, DLB, and less frequently AD. The aims of this study are: (i) to assess brain glucose metabolism measured by [18F]FDG PET in patients affected by iRBD compared to a group of healthy controls; (ii) to compare the [18F]FDG uptake of iRBD patients to different groups of patients affected by neurodegenerative disorders such as PD, DLB, AD.

2. Methods

2.1. Participants and study design

We studied patients affected by iRBD, PD, DLB, and AD admitted to the Neurology Clinic of the University of Rome “Tor Vergata” or IRCSS Neuromed. All patients underwent [18F]FDG PET in order to evaluate brain glucose consumption. All patients received the diagnosis according to the current version of the diagnostic guidelines for each disorder. In particular, iRBD was diagnosed according to the guidelines present in the International Classification of Sleep Disorders and based on video-polysomnographic recording [1]; AD was diagnosed according to McKhann et al. criteria [13]; DLB was defined as McKheit et al. guidelines [14]; idiopathic PD according to the UK Parkinson's Disease Society Brain Bank criteria [15]. All iRBD, PD, DLB, and AD patients were drug-naïve since the [18F]FDG PET study was performed during the diagnostic standard protocol at the Neurology Clinics. We also included a group of control subjects, which has been previously described [16]. Briefly, controls were chemotherapy naïve subjects undergoing a [18F]FDG PET evaluation, which resulted completely negative, showing a MMSE > 27/30 and not using drugs active on CNS.

Exclusion criteria for patients and controls were the following: systemic and/or neurologic infectious, inflammatory or autoimmune diseases; diabetes; concomitant psychiatric or other neurological disorders; previous history of stroke or cerebral infarctions documented in magnetic resonance imaging (MRI). In particular, we included in the iRBD group exclusively patients affected by RBD and not showing a possible iatrogenic cause of the sleep disorder or concomitant neurological/psychiatric diseases.

The study protocol was considered as observational by the internal review board of the Local Ethical Committee and performed according to the STROBE statement.

2.2. [18F]FDG PET scanning

The PET/CT system Discovery VCT (GE Medical Systems, Tennessee, USA) has been used to assess brain distribution of [18F]FDG in all the subjects by means of a 3Dmode standard technique with the same imaging modalities reported previously by our group in agreement with standard guidelines [14]. In particular, all the subjects fasted for at least 5 h before intravenous injection of [18F]FDG (dose range 185–250 Mega Becquerels); the serum glucose level was less or equal than 108 mg/ml in all subjects. A static scan has been performed 30 min after the injection of the radiolabeled compound. Reconstruction method for PET scan included ordered Subsets Expectation Maximization Algorithm (20 iterations, 4 subsets) with a 256 × 256 matrix. Drugs that have been reported to interfere with [18F]FDG bio distribution were discontinued in all the subjects examined.

2.3. Data analysis

2.3.1. Analysis of [18F]FDG PET data in patients and control groups

We used statistical parametric mapping (SPM8, Wellcome Department of Cognitive Neurology, London, UK) implemented in MATLAB 2016b (MathWorks, Natick, MA, USA) for biodistribution analysis in the brain for both radiolabeled compounds. [18F]FDG PET data were subjected to affine and non-linear spatial normalization into the Montreal Neurological Institute space (MNI) with a dementia-specific [18F]FDG PET template for SPM normalization ([17]). We applied an 8-mm isotropic Gaussian filter to blur the individual variations (especially gyral variations) and increase the signal-to-noise ratio. We used the following parameters and post processing tools before *t*-test regression analysis was applied: global normalization, 50 (using proportional scaling); masking threshold, 0.8; transformation tool of statistical parametric maps into normal distribution; correction of SPM coordinates to match the Talairach coordinates, subroutine implemented by Matthew Brett (http://www.mrc-cbu.cam.ac.uk/Imaging). Brodmann areas (BA) were identified at a range from 0 3 mm from the corrected Talairach coordinates of the SPM output isocenter by using a Talairach client available http://www.talairach.org/index.html. As proposed by Bennett et al. [18], SPM t-maps have been corrected for multiple comparisons with the false discovery rate (P = 0.05) and corrected for multiple comparisons at cluster level (P = 0.001). Only those clusters containing more than 100 (5 × 5 × 5 voxels, i.e., 11 × 11 × 11 mm) contiguous voxels were considered significant.

For the comparison among groups, the voxel-based analysis was performed using a modality-adjusted paired *t*-test (two conditions, one scan/condition) and the following comparisons were assessed: iRBD vs PD, iRBD vs DLB, iRBD vs AD, iRBD vs controls, using sex, age, and MMSE as nuisance variables. We also performed a secondary analysis

Table 2
Differences in cortical [18F]FDG consumption in iRBD vs. Controls, PD, DLB, and AD.

Analysis	Cluster level				Voxel level		
Comparison	clusterp(FWE-corr)	Cluster p(FDR-corr)	Cluster extent	Cortical Region	Z score of maximum	Talairach coordinates	Cortical region
iRBD-Controls (increased [18F]FDG uptake in brain areas of iRBD compared to controls)	*< 0.001*	< 0.001	3248	R Temporal lobe, inferior temporal gyrus	6.14	30,-6,-44	BA20
				R Brainstem, medulla	5.72	2,-20,-38	–
				L Brainstem, medulla	5.22	−2,-30,-36	-
	< 0.001	< 0.001	1450	R Parahippocampal gyrus, hippocampus	6.1	32,-12,-12	-
				R Temporal lobe, fusiform gyrus	5.32	42,-4,-20	BA20
				R Temporal lobe, middle temporal gyrus	4.32	54,-20,-18	BA21
	0.005	0.007	571	R Limbic lobe, anterior cingulate	5.97	14,44,4	BA10
				R Frontal lobe, medial frontal gyrus	5.48	14,38,16	BA9
	< 0.001	< 0.001	2230	L Limbic lobe, uncus	5.62	−24,-12,-38	BA36
				L Limbic lobe, hippocampus	5.40	−30,-14,-12	–
	0.022	0.020	405	L Frontal lobe, middle frontal gyrus	4.87	−34,54,-14	BA11
Controls – iRBD (reduced [18F]FDG uptake in brain areas of iRBD compared to controls)	*< 0.001*	< 0.001	4485	R Parietal lobe, precuneus	5.99	2,-72,34	BA7
				L Superior parietal lobule	4.68	−40,-76,48	BA7
				L Parietal lobe, precuneus	4.47	−26,-86,46	BA19
	< 0.001	< 0.001	2343	R Occipital lobe, cuneus	5.29	34,-88,36	BA19
				R Temporal lobe, middle temporal gyrus	5.14	64,-66,0	BA37
iRBD-PD (increased [18F]FDG uptake in brain areas of iRBD compared to PD)	*< 0.001*	< 0.001	1186	R Brainstem, pons	5.93	2,-20,-34	–
				R Brainstem, pons	5.78	2,-30,-32	–
				R Brainstem, midbrain	4.11	10,-20,-12	–
	0.003	0.006	749	Left Frontal lobe, middle frontal gyrus	5.21	−44,40,-14	BA11
				Left Frontal lobe, inferior frontal gyrus	4.1	−44,40,-14	BA11
				Left Frontal lobe, inferior frontal gyrus	3.69	−32,26,0	BA47
	< 0.001	< 0.001	1594	Left Temporal lobe, fusiform gyrus	5.52	−58,-18,-22	BA20
				Left Temporal lobe, inferior temporal gyrus	5.11	−56,-30,-18	BA20
				Left Temporal lobe, fusiform gyrus	4.97	−52,-40,-22	BA20
	0.043	0.036	380	R Lentiform nucleus, putamen	4.83	20,16,-6	–
				R Lentiform nucleus, putamen	4.35	28,8,-4	–
				R Claustrum	3.61	34,-10,-8	–
	0.005	0.007	674	R Frontal lobe, inferior frontal gyrus	4.32	52, 34, −2	BA47
				R Frontal lobe, inferior frontal gyrus	4.31	50, 32, −10	BA47
iRBD – DLB (increased [18F]FDG uptake in brain areas of iRBD compared to DLB)	*0.002*	0.003	697	R Occipital lobe, lingual gyrus	4.51	22,-102,-10	BA17
				R Occipital lobe, cuneus	4.15	14,-102,2	BA18
				R Occipital lobe, cuneus	4.10	20,-96,22	BA19
	< 0.001	< 0.001	1885	R Parietal lobe, precuneus	4.40	10,-68,48	BA7
				R Occipital lobe, cuneus	4.00	16,-70,32	BA7
				R Parietal lobe, superior parietal lobule	3.91	16,-66,58	BA7
	0.001	0.002	866	R Temporal lobe, fusiform gyrus	4.73	50, −54, −18	BA37
				R Temporal lobe, fusiform gyrus	4.45	60,-50,-18	BA37
				R Temporal lobe, middle temporal gyrus	4.41	50,-70,4	BA37
DLB-iRBD(reduced [18F]FDG uptake in brain areas of iRBD compared to DLB)	*0.002*	0.004	704	R Limbic lobe, anterior cingulate	4.40	14,28,-10	BA32
				R Limbic lobe, anterior cingulate	4.02	−12,28,-10	BA32
				L frontal lobe, subcallosal gyrus	3.86	−4,16,-14	BA25
iRBD-AD (increased [18F]FDG uptake in brain areas of iRBD compared to AD)	< 0.001	< 0.001	1824	L Limbic lobe, cingulate gyrus	5.24	−4,-38,34	BA31
				L Parietal lobe, precuneus	4.98	−6,-50,34	BA31
				R Parietal lobe, precuneus	4.72	−6,-50,34	BA31
	0.001	0.002	998	L Temporal lobe, inferior temporal gyrus	4.60	−42,-18,-34	BA20
				L Temporal lobe, inferior temporal gyrus	4.45	−40,-12,-42	BA20

(*continued on next page*)

Table 2 (*continued*)

Analysis	Cluster level			Voxel level			
Comparison	clusterp(FWE-corr)	Cluster p(FDR-corr)	Cluster extent	Cortical Region	Z score of maximum	Talairach coordinates	Cortical region
AD-iRBD (reduced [18F]FDG uptake in brain areas of iRBD compared to AD)	0.019	0.037	529	L Frontal lobe, middle frontal gyrus	4.99	− 30,36,-2	BA11
				L Frontal lobe, middle frontal gyrus	4.20	− 16,50,10	BA10
				L Frontal lobe, middle frontal gyrus	3.93	− 22,26,-10	BA11
	0.017	0.037	546	R Frontal lobe, middle frontal gyrus	4.51	30,36,-2	BA11
				R Frontal lobe, superior frontal gyrus	4.37	20,52,6	BA10
				R Frontal lobe, middle frontal gyrus	4.26	28,36,-4	BA11

comparing controls to AD, DLB and PD patients using sex, age, and MMSE as nuisance variables in order to test the [18F]FDG uptake in each neurodegenerative disorder. In the SPM maps, we searched the brain areas with a significant correlation using a statistical threshold of P = 0.001, family wise error corrected for the problem of multiple comparisons, with an extent threshold of 100 voxels.

3. Results

We included in this study 54 iRBD, 28 PD, 10 DLB, 55 AD, and 35 controls. Demographic and clinical features of patients and controls are summarized in Table 1.

Considering [18F]FDG PET analysis, for clarity we report in this section the comparison between iRBD patients to PD, DLB, AD and controls.

When comparing iRBD to controls, we documented that iRBD patients showed glucose relative hypometabolism in a wide cluster including BA 7, 19, and 37, owing to precuneus, superior parietal lobule and middle temporal gyrus (see Table 2 and Fig. 1). Conversely, iRBD patients showed increased FDG uptake in several BAs compared to controls, owing to temporal lobe, limbic lobe, and frontal lobe and in the brainstem (see Table 2 and Fig. 1).

Thereafter, we compared iRBD patients to patients affected by different neurodegenerative processes. When comparing iRBD to PD group, we documented that iRBD patients showed increased FDG uptake compared to PD patients in the midbrain and pons, cerebellum, lentiform nucleus and claustrum, and in frontal and temporal lobes (see Table 2 and Fig. 2). Conversely, PD patients did not show areas with increased FDG uptake compared to iRBD patients. Considering the AD and DLB groups, when comparing iRBD to DLB group we documented that iRBD patients showed increased FDG uptake in temporal, parietal, and occipital lobes than DLB, whereas iRBD patients showed glucose relative hypometabolism compared to DLB patients in frontal and limbic lobes (see Table 2 and Fig. 3). Finally, iRBD patients showed reduced FDG uptake in the frontal lobe and increased FDG uptake in limbic, temporal and parietal lobes compared to AD patients (see Table 2 and Fig. 4).

Finally, we compared the control group to AD, PD and DLB groups; concerning the comparison between controls and AD patients, the reduction of brain glucose consumption in a wide cluster that included temporal, parietal, limbic and frontal lobes was evident in AD (see Table 3). Comparing controls to DLB patients the reduction of brain glucose consumption in parietal, occipital (BA19) and frontal regions was evident in DLB. The comparison between controls and PD patients showed the reduced [18F]FDG uptake in parietal and limbic cortices in PD (Table 3).

4. Discussion

In the present study we showed that patients affected by iRBD present a distinct cerebral glucose consumption featured by increased FDG uptake in the brainstem and in the limbic, temporal and frontal lobes compared to controls. In particular, the brain [18F]FDG uptake showed by iRBD patients is different from the other neurodegenerative disorders, such as AD, PD, and DLB. iRBD patients also presented a significant glucose relative hypometabolism in crucial areas for memory and cognitive functions, such as precuneus, superior parietal lobule and middle temporal gyrus, which are brain regions frequently altered in the early stages of neurodegeneration [10–12]. Moreover, iRBD patients showed relative increased cerebral glucose metabolism in brainstem, which contains centers regulating the sleep-wake cycle [19]. Although several studies compared brain [18F]FDG PET of iRBD patients to controls in the recent years [10–12], the novelty of the present study is the comparison among iRBD, PD, DLB, AD, and controls.

[18F]FDG PET investigates the resting-state cerebral metabolic rate of glucose and it has been appropriately chosen for better

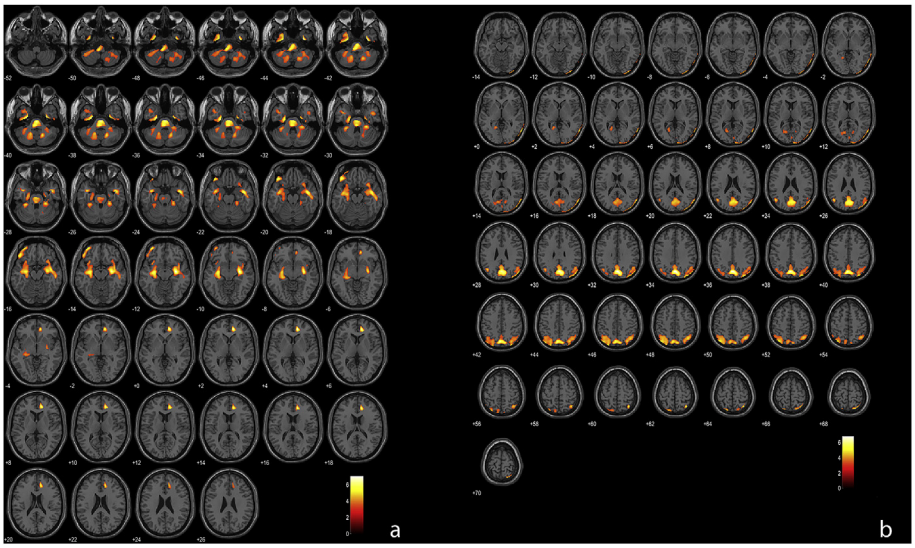

Fig. 1. Overlay of the SPM results comparison reported in Table 2 (iRBD-controls and controls-iRBD) with a T1 magnetic resonance template available in SPM showing in (a) the increased [18F]FDG uptake in the brainstem, temporal, limbic and frontal lobes and (b) the reduced [18F]FDG uptake in parietal and occipital lobes in iRBD patients.

understanding the underlying neurodegenerative processes of PD, DLB and AD [20]. Moreover, [18F]FDG PET has been widely applied in neurodegenerative disorders since it allows the identification of cerebral glucose relative hypometabolism predicting brain atrophy in different forms of dementia [21]. Accordingly, during the past years [18F]FDG PET has been largely used to study the physiopathology of several neurodegenerative disorders. In AD, a specific [18F]FDG PET pattern has been identified and actually represents one of the biomarkers for AD diagnosis [13]. In particular, in the early stages of the AD process, cerebral glucose relative hypometabolism is commonly observed in the parietal and temporal cortices, posterior cingulate cortex, and precuneus. As the disease progresses, the AD pathology spreads to involve the frontal cortex, whereas the metabolism in the striatum, thalamus, primary sensorimotor cortex, visual cortex, and cerebellum is relatively preserved [22]. In DLB, it has been demonstrated a prevalent synaptic dysfunction and neurotransmission dysregulation recognized by [18F]FDG PET in the posterior brain cortical areas [23]. Nevertheless, in patients affected by DLB, the [18F]FDG PET studies frequently show generalized decreased glucose consumption, with higher relative hypometabolism in both occipital and parietal regions [23]. This peculiar pattern of [18F]FDG uptake appears to have good sensitivity in distinguishing DLB from AD [22], where the relative sparing of the glucose metabolism in the visual cortex is present. Finally, a PD related pattern (PDRP) identifiable in [18F]FDG PET has been designed in studies performed in PD patients [25]. Accordingly, PD patients show glucose relative hypermetabolism in pallido-thalamic, pontine, and cerebellar regions, associated with concurrent glucose relative hypometabolism in the premotor, temporal and posterior parietal areas, which mainly represent the neurons' circuitries disconnection and neurodegeneration in those specific brain areas, also associated with reduced performances in attention and memory-based tasks [24,26]. However, PD patients may show a preserved [18F]FDG uptake in the striatal regions, and this preservation of the metabolic activity in the basal ganglia may allow the differentiation from other parkinsonian syndromes, such as MSA and progressive supranuclear palsy [23,27,28].

Concomitant with the identification of the PDRP pattern in PD patients, also in iRBD patients a specific pattern of [18F]FDG has been very recently hypothesized [10,11]. It is named iRBD-related pattern (iRBDRP) and consists of increased glucose relative metabolism in cerebellum, brainstem, thalamus, sensorimotor cortex, and hippocampus, and of glucose relative hypometabolism in middle cingulate, temporal, occipital and parietal cortices [10,11]. This iRBDRP partially overlaps with the PDRP and may be an early manifestation of this specific pattern present in PD patients. In the present study, we did not document significant differences in [18F]FDG uptake in iRBD patients when compared to PD. This finding partially overlaps with the previous literature reports confirming that iRBD present a similar [18F]FDG uptake pattern compared to PD [10,11]. We are aware that iRBD patients may convert in different neurodegenerative disorders, and predominantly in α-synucleinopathies [5]. In agreement with these results, iRBD patients frequently convert to PD and DLB and less frequently to MSA, mild cognitive impairment or AD [5]. Since the already demonstrated longitudinal phenoconversion of iRBD patients at follow-up [5], studies aimed at identifying the best instrument able to predict the phenoconversion of iRBD patients to a specific neurodegenerative process are actually invoked in order to set possible preventive strategies against neurodegeneration.

In this study, we compared [18F]FDG PET images of iRBD patients to four different groups. Accordingly, we did not exclusively compare neuroimages of iRBD patients to controls, but we would test whether the brain glucose metabolism of iRBD patients may overlap or differ from that presented by PD, DLB, or AD patients. Although we are aware of a possible limitation of the analysis due to the lower number of patients included in the DLB and in the PD groups, the novel finding of this report is the significant differences found in cerebral [18F]FDG uptake of iRBD patients compared to all groups (controls, PD, DLB, and AD). As expected, the main differences were found between iRBD and AD patients, thus providing a further evidence of a different neurodegenerative process underlying iRBD condition, which does not resemble that of AD pathology. In agreement with the present findings, the majority of longitudinal investigations do not report AD as a possible development for patients affected by iRBD and our results agree with this literature evidence [7]. Therefore, this finding concords with the literature suggestion that iRBD can represent a prodromal manifestation of α-synucleinopathies and not tauopathies. Moreover, another limitation of our study is the lack of an appropriate correction for gray matter ratio (GMR), which is the percentage of the gray matter volume divided by the intracranial volume. Considering the exploratory aspect of our study and that it is mainly directed to the study of glucose metabolism in different neurodegenerative disorders, magnetic resonance imaging was exclusively used for diagnostic purposes. Future studies, possibly on a larger cohort of patients, should also include GMR in the analyses. Finally, we are aware that the use of overall grand mean scaling for counts may lead to normalization artifacts in global mean normalization; nevertheless scaling of the overall grand mean easily scales all the data by a common factor with no effects on the statistical analysis but just changing the unit of measure. For this reason, although it can limit our results, the impact of overall grand mean scaling has a scarce

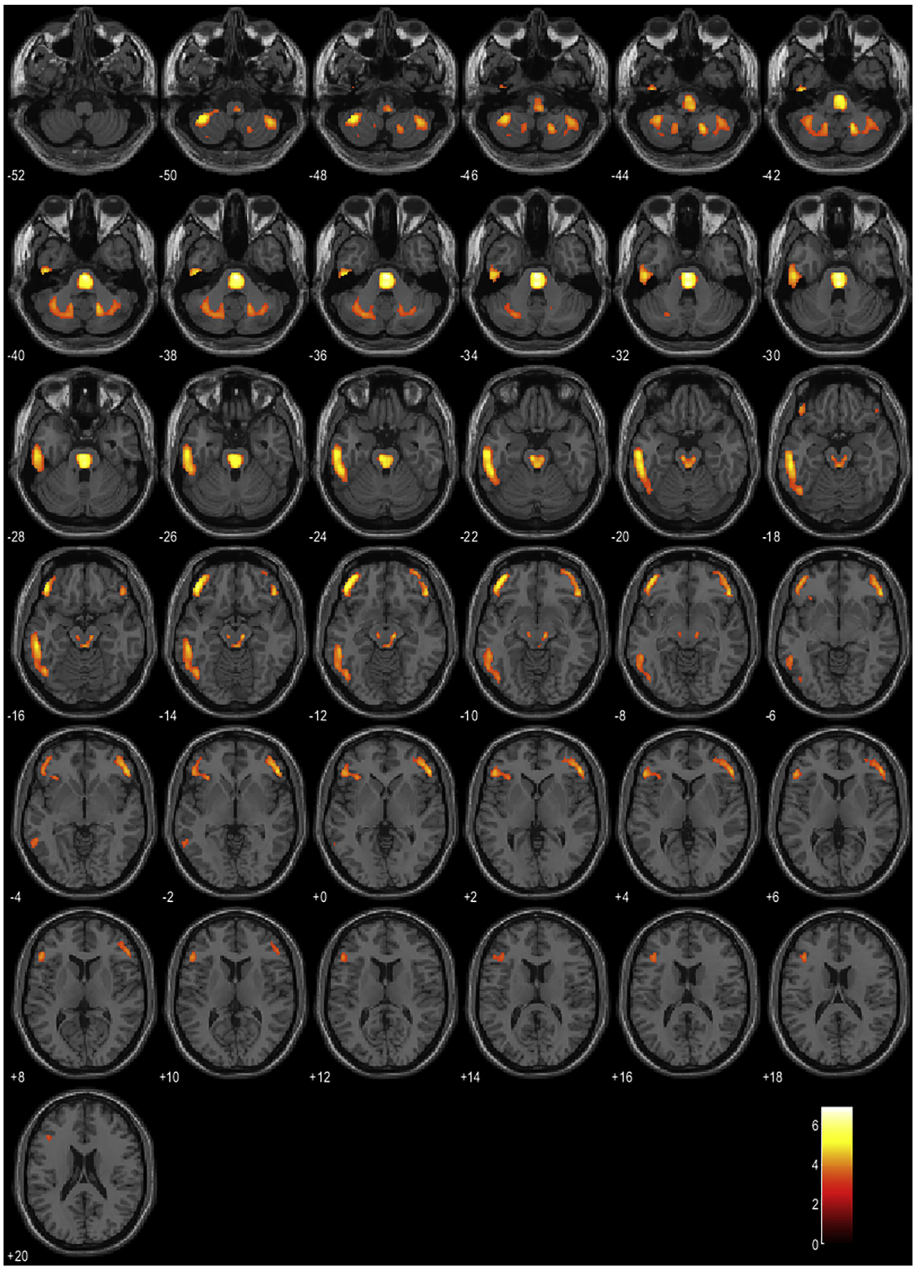

Fig. 2. Overlay of the SPM results comparison reported in Table 2 (iRBD-PD) with a T1 magnetic resonance template available in SPM showing the increased [18F] FDG uptake in temporal and frontal lobes and in brainstem in iRBD patients.

effect on the significance of the analysis performed.

In keeping with our results, it is actually demonstrated that patients affected by iRBD do not show a peculiar cerebral glucose metabolism. In fact, clinicians do not currently have instruments for predicting the time of phenoconversion to a specific neurodegenerative disorder in iRBD patients. It has been hypothesized that there is a sort of LB disease related pattern at [18F]FDG PET, with a progressive degree for severity from iRBD, to PD and eventually to DLB [10]. Moreover, the heterogeneous cerebral spreading of α-synuclein pathology and its interaction with concomitant genetic factors, cognitive reserve, and brain pathologies might largely explain the different rates of conversion of iRBD patients in longitudinal cohorts [5]. Therefore, the evolution of the neurodegenerative process underlying iRBD condition is hard to detect and nowadays we did not have possibilities to predict the time and way of phenoconversion. The alteration of [18F]FDG PET has been only hypothesized as a possible early biomarker of conversion in iRBD patients, since a previous cross-sectional study demonstrated that [18F] FDG PET, combined with dopamine transporter binding and olfaction, may complementary provide information for predicting phenoconversion [28]. Moreover, latent network abnormalities detected by [18F] FDG PET in iRBD patients have been associated with a greater likelihood of subsequent phenoconversion to a progressive α-synucleinopathy [12,29].

Notably, this study confirmed the alteration of brain [18F]FDG uptake in iRBD patients. Indeed, iRBD patients present an abnormal relative glucose metabolism in brainstem, precuneus, temporal and limbic regions, and frontal cortex (see Table 2). There may be a way to explain this finding. Considering that: i) brainstem contains nuclei regulating REM sleep [19], ii) precuneus and frontal lobe control behavioral symptoms [30], iii) temporal and limbic regions regulate cognitive functions [31]. Hence, the documented alterations of these brain areas may reflect sleep, behavioral and cognitive symptoms

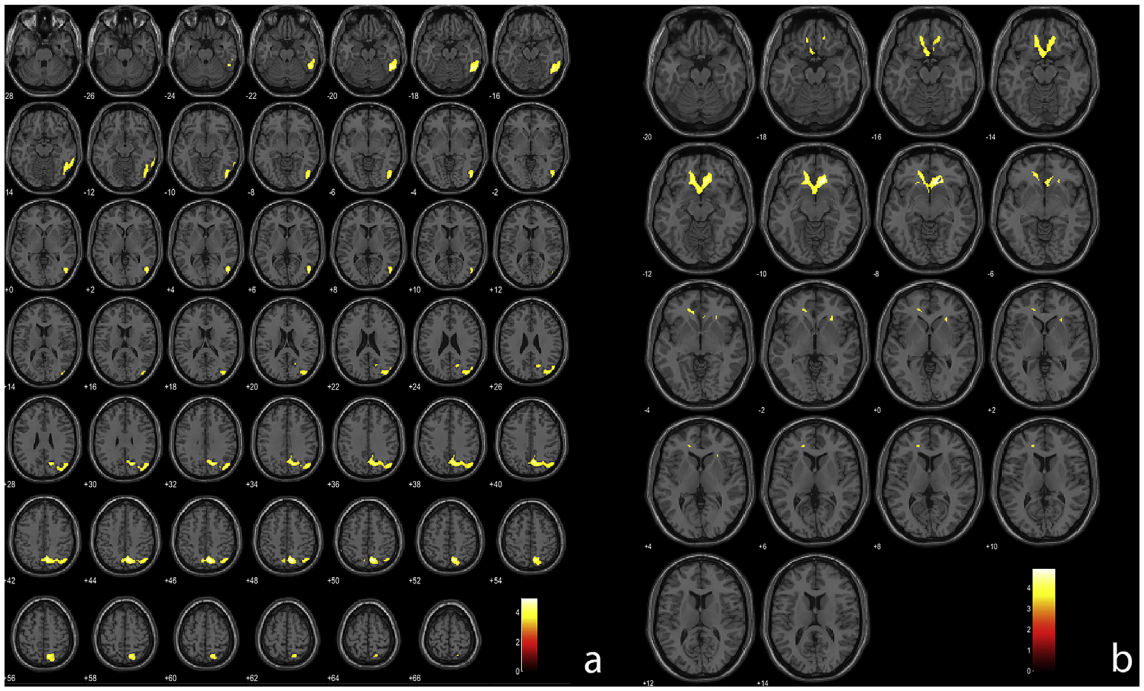

Fig. 3. Overlay of the SPM results comparison reported in Table 2 (iRBD-DLB and DLB-iRBD) with a T1 magnetic resonance template available in SPM showing in (a) the increased [18F]FDG uptake in occipital, parietal and temporal lobes, and (b) the decrease [18F]FDG uptake in limbic and frontal lobes in iRBD patients.

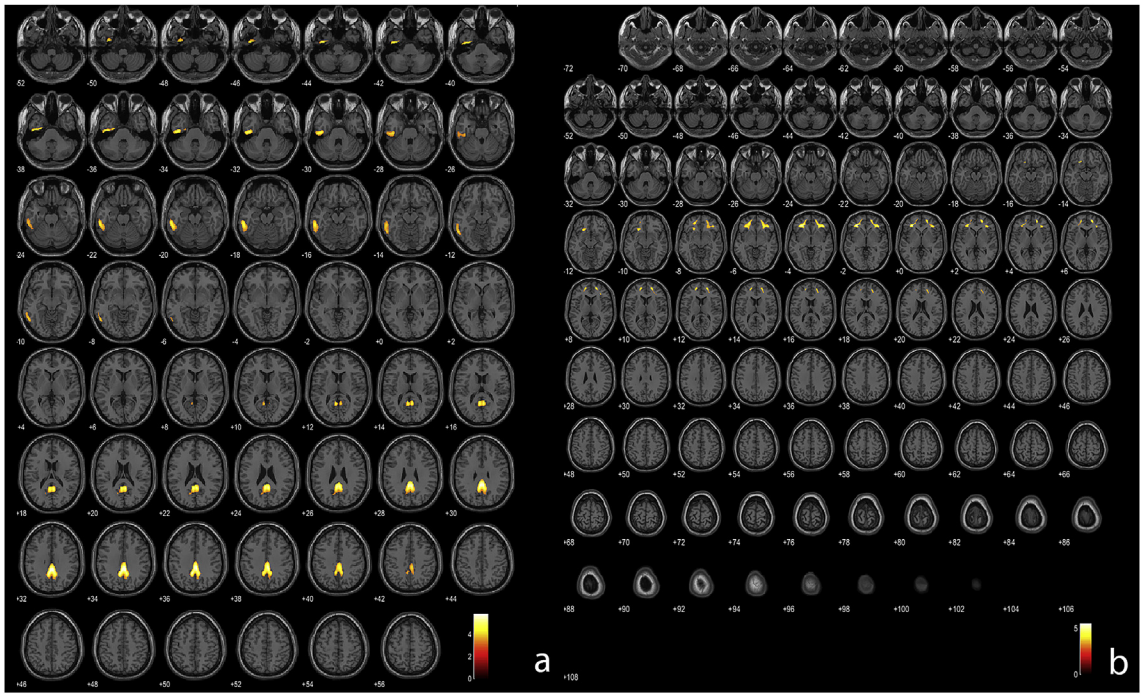

Fig. 4. Overlay of the SPM results comparison reported in Table 2 (iRBD-AD and AD-iRBD) with a T1 magnetic resonance template available in SPM showing in (a) the increased [18F]FDG uptake in limbic, parietal end temporal lobes and (b) the reduced [18F]FDG uptake in frontal lobes in iRBD patients.

present in iRBD patients and due to the initial deposition of α-synuclein in LB, also taking into account the Braak hypothesis proving that α-synuceinopathy starts in the brainstem and longitudinally diffuses to the cortical brain regions [32].

5. Conclusion

In conclusion, we suggest that neuronal energy glucose damage occurs in iRBD patients, and may be the possible expression of the neurodegenerative processes already affecting these patients. In agreement with our hypothesis, recent evidence showed that all iRBD patients exhibit signs and symptoms of neurodegeneration [33]. Notably, the present study further supports the hypothesis that AD pathology can not induce RBD manifestations, since the documentation of significant differences in the cerebral [18F]FDG uptake presented by iRBD when compared to AD patients.

Hence, considering that brain metabolism is a reliable marker of local synaptic and neural dysfunction, which often precedes by many

Table 3
Differences in cortical [18F]FDG uptake in AD, DLB and PD vs controls.

Analysis	Cluster level					Voxel level	
Comparison	Cluster p(FWE-corr)	Cluster p(FDR-corr)	Cluster extent	Cortical Region	Z score of maximum	Talairach coordinates	Cortical region
Controls – AD (reduced [18F]FDG uptake in brain areas of AD compared to controls)	< 0.001	< 0.001	30388	R Temporal lobe, superior temporal gyrus	7.63	46,-59,31	BA39
				R Parietal lobe, precuneus	7.52	8,-60,32	BA7
				R Temporal lobe, parahippocampal gyrus	7.50	6,-68,34	BA7
	< 0.001	< 0.001	18153	L Frontal lobe, superior frontal gyrus	6.90	−6,-50,32	BA9
				R Limbic lobe, cingulate gyrus	6.76	4,-42,34	BA31
				R Limbic lobe, cingulate gyrus	6.60	4,-28,36	BA31
	< 0.001	< 0.001	3097	R Frontal lobe, superior frontal gyrus	4.79	28,26,54	BA8
				R Frontal lobe, middle frontal gyrus	4.33	36,14,54	BA6
				R Frontal lobe, middle frontal gyrus	4.25	34,26,42	BA8
	< 0.001	< 0.001	30017	R Parietal lobe, superior parietal lobule	5.74	8,-68,52	BA7
				R Parietal lobe, precuneus	5.73	6,-64,38	BA7
				R Parietal lobe, precuneus	5.70	46,-74,40	BA19
				R Frontal lobe, middle frontal gyrus	4.54	54,24,36	BA9
				R Frontal lobe, middle frontal gyrus	3.77	14,32,56	BA9
				R Frontal lobe, middle frontal gyrus	3.63	34,18,58	BA6
Controls – DLB (reduced [18F]FDG uptake in brain areas of DLB compared to controls)	< 0.001	< 0.001	18843	R Frontal lobe, middle frontal gyrus	3.63	34,18,58	BA6
				R Limbic lobe, posterior cingulate	5.08	8,-58,14	BA23
				R Parietal lobe, precuneus	4.85	−10,-76,54	BA7
				R Parietal lobe, precuneus	4.84	−8,-58,42	BA7
	< 0.001	< 0.001	2343	R Occipital lobe, cuneus	5.29	34,-88,36	BA19
				R Temporal lobe, middle temporal gyrus	5.14	64,-66,0	BA37
Controls – PD (reduced [18F]FDG uptake in brain areas of PD compared to controls)	< 0.001	< 0.001	3340	L limbic lobe, posterior cingulate	5.08	8,-58,14	BA32
				R Parietal lobe, precuneus	4.85	10,-76,54	BA7
				L Parietal lobe, precuneus	4.84	−8,-58,-42	BA7

years structural damage and clinical signs of neurodegeneration [34], we highlight the need for understanding the neuronal mechanisms accounting for brain metabolism alteration in iRBD patients in order to potentially identify iRBD subtypes and set new strategies and approaches to counteract neuronal damage and predict the phenoconversion to specific LB neurodegenerative disorders and thus possibly start the most appropriate neuroprotective treatment strategy.

Compliance with Ethical Standards

Funding and conflict of interest

Claudio Liguori, Agostino Chiaravalloti, Roberta Ruffini, Alessandro Stefani, Enrica Olivola, Orazio Schillaci, Nicola Modugno, Diego Centonze Nicola Biagio Mercuri, Fabio Placidi report no financial disclosures/fundings or conflict of interest related to this work.

Ethical approval

All procedures performed in studies involving human participants were in accordance with the ethical standards of the institutional and/or national research committee and with the 1964 Helsinki declaration and its later amendments or comparable ethical standards.

Informed consent

Informed consent was obtained from all individual participants included in the study.

References

[1] International Classification of Sleep Disorders, third ed., American Academy of sleep medicine, Darien, IL, 2014.
[2] Y.E. Ju, Rapid eye movement sleep behavior disorder in adults younger than 50 years of age, Sleep Med. 14 (8) (2013) 768–774.
[3] Y.E. Ju, L. Larson-Prior, S. Duntley, Changing demographics in REM sleep behavior disorder: possible effect of autoimmunity and antidepressants, Mar, Sleep Med. 12 (3) (2011) 278–283.
[4] B.F. Boeve, REM sleep behavior disorder: updated review of the core features, the REM sleep behavior disorder-neurodegenerative disease association, evolving concepts, controversies, and future directions, Ann. N. Y. Acad. Sci. 1184 (2010) 15–54.
[5] C.H. Schenck, B.F. Boeve, M.W. Mahowald, Delayed emergence of a parkinsonian disorder or dementia in 81% of older men initially diagnosed with idiopathic rapid eye movement sleep behavior disorder: a 16-year update on a previously reported series, Aug, Sleep Med. 14 (8) (2013) 744–748.
[6] M.G. Spillantini, R.A. Crowther, R. Jakes, M. Hasegawa, M. Goedert, α-Synuclein in filamentous inclusions of Lewy bodies from Parkinson's disease and dementia with Lewy bodies, Proc. Natl. Acad. Sci. U. S. A. 95 (11) (1998) 6469–6473.
[7] A. Galbiati, G. Carli, M. Hensley, L. Ferini-Strambi, REM sleep behavior disorder and alzheimer's disease: definitely No relationship? J. Alzheimer's Dis. 63 (1) (2018) 1–11.
[8] L. Moscoli, Glucose metabolism in normal aging and Alzheimer's disease: methodological and physiological considerations for PET studies, Aug, Clin. Transl. Imag. 1 (4) (2013).
[9] A. Varrone, S. Asenbaum, T. Vander Borght, J. Booij, F. Nobili, K. Någren, et al., European Association of Nuclear Medicine Neuroimaging Committee. EANM procedure guidelines for PET brain imaging using [18F]FDG, version 2, Dec, Eur. J. Nucl. Med. Mol. Imaging 36 (12) (2009) 2103–2110.
[10] S.K. Meles, R.J. Renken, A. Janzen, D. Vadasz, M. Pagani, D. Arnaldi, et al., The metabolic pattern of idiopathic REM sleep behavior disorder reflects early-stage Parkinson's disease, J. Nucl. Med. (2018), https://doi.org/10.2967/jnumed.117.202242.
[11] P. Wu, H. Yu, S. Peng, Y. Dauvilliers, J. Wang, J. Ge, et al., Consistent abnormalities in metabolic network activity in idiopathic rapid eye movement sleep behaviour disorder, Brain 137 (12) (2014) 3122–3128.
[12] F. Holtbernd, J.F. Gagnon, R.B. Postuma, Y. Ma, C.C. Tang, A. Feigin, et al., Abnormal metabolic network activity in REM sleep behavior disorder, Neurology 82 (7) (2014) 620–627.
[13] G.M. McKhann, D.S. Knopman, H. Chertkow, B.T. Hyman, C.R. Jack Jr., C.H. Kawas, et al., The diagnosis of dementia due to Alzheimer's disease: recommendations from the National Institute on Aging-Alzheimer's Association workgroups on diagnostic guidelines for Alzheimer's disease, Alzheimer's Dementia 7 (3) (2011) 263–269.
[14] I.G. McKeith, B.F. Boeve, D.W. Dickson, G. Halliday, J.P. Taylor, D. Weintraub, et al., Diagnosis and management of dementia with Lewy bodies: fourth consensus report of the DLB consortium, Neurology 89 (1) (2017) 88–100.
[15] A.J. Hughes, S.E. Daniel, L. Kilford, A.J. Lees, Accuracy of clinical diagnosis of idiopathic Parkinson's disease: a clinico-pathological study of 100 cases, J. Neurol. Neurosurg. Psychiatry 55 (3) (1992) 181–184.
[16] C. Liguori, A. Chiaravalloti, G. Sancesario, A. Stefani, G.M. Sancesario, N.B. Mercuri, et al., Cerebrospinal fluid lactate levels and brain [18F]FDG PET hypometabolism within the default mode network in Alzheimer's disease, Eur. J. Nucl. Med. Mol. Imaging 43 (11) (2016) 2040–2049.
[17] D. Perani, P.A. Della Rosa, C. Cerami, F. Gallivanone, F. Fallanca, E.G. Vanoli, et al., Validation of an optimized SPM procedure for FDG-PET in dementia diagnosis in a clinical setting, Neuroimage Clin. 24 (6) (2014) 445–454.
[18] C.M. Bennett, G.L. Wolford, M.B. Miller, The principled control of false positives in neuroimaging, Soc. Cognit. Affect Neurosci. 4 (4) (2009) 417–422.
[19] T.E. Scammell, E. Arrigoni, J.O. Lipton, Neural circuitry of wakefulness and sleep, Neuron 93 (4) (2017) 747–765.
[20] K. Herholz, PET studies in dementia, Ann. Nucl. Med. 17 (2) (2003) 79–89.
[21] R. González-Redondo, D. García-García, P. Clavero, C. Gasca-Salas, R. García-Eulate, J.L. Zubieta, et al., Grey matter hypometabolism and atrophy in Parkinson's disease with cognitive impairment: a two-step process, Brain 137 (Pt8) (2014) 2356–2367.
[22] K. Ishii, PET approaches for diagnosis of dementia, AJNR Am. J. Neuroradiol. 35 (11) (2014) 2030–2038.
[23] P. Zhao, B. Zhang, S. Gao, 18F-FDG PET study on the idiopathic Parkinson's disease from several parkinsonian-plus syndromes, Park. Relat. Disord. 18 (Suppl 1) (2012) S60–2.
[24] M.J. Firbank, A.J. Yarnall, R.A. Lawson, G.W. Duncan, T.K. Khoo, G.S. Petrides, et al., Cerebral glucose metabolism and cognition in newly diagnosed Parkinson's disease: ICICLE-PD study, Apr, J. Neurol. Neurosurg. Psychiatry 88 (4) (2017) 310–316.
[25] D. Eidelberg, Metabolic brain networks in neurodegenerative disorders: a functional imaging approach, Oct, Trends Neurosci. 32 (10) (2009) 548–557.
[26] P. Wu, J. Wang, S. Peng, Y. Ma, H. Zhang, Y. Guan, et al., Metabolic brain network in the Chinese patients with Parkinson's disease based on 18F-FDG PET imaging, Park. Relat. Disord. 19 (6) (2013) 622–627.
[27] C.C. Tang, K.L. Poston, T. Eckert, A. Feigin, S. Frucht, M. Gudesblatt, et al., Differential diagnosis of parkinsonism: a metabolic imaging study using pattern analysis, Lancet Neurol. 9 (2) (2010) 149–158.
[28] T. Eckert, A. Barnes, V. Dhawan, S. Frucht, M.F. Gordon, A.S. Feigin, et al., FDG PET in the differential diagnosis of parkinsonian disorders, Neuroimage 26 (3) (2005) 912–921.
[29] S.K. Meles, D. Vadasz, R.J. Renken, E. Sittig-Wiegand, G. Mayer, C. Depboylu, et al., FDG PET, dopamine transported SPECT, and olfaction: combining biomarkers in REM sleep behavior disorder, Mov. Disord. 32 (10) (2017) 1482–1486.
[30] H.J. Rosen, S.C. Allison, G.F. Schauer, M.L. Gorno-Tempini, M.W. Weiner, B.L. Miller, Neuroanatomical correlates of behavioural disorders in dementia, Brain 128 (Pt 11) (2005) 2612–2625.
[31] K. Kantarci, S.D. Weigand, S.A. Przybelski, G.M. Preboske, V.S. Pankratz, P. Vemuri, et al., MRI and MRS predictors of mild cognitive impairment in a population-based sample, Neurology 81 (2) (2013) 126–133.
[32] H. Braak, K. Del Tredici, U. Rüb, R.A. de Vos, E.N. Jansen Steur, E. Braak, Staging of brain pathology related to sporadic Parkinson's disease, Neurobiol. Aging 24 (2) (2003) 197–211.
[33] C. Yao, S.M. Fereshtehnejad, B.K. Dawson, A. Pelletier, Z. Gan-Or, J.F. Gagnon, et al., Longstanding disease-free survival in idiopathic REM sleep behavior disorder: is neurodegeneration inevitable? Park. Relat. Disord. 54 (2018 Sep) 99–102, https://doi.org/10.1016/j.parkreldis.2018.04.010.
[34] D. Perani, J. Abutalebi, Bilingualism, dementia, cognitive and neural reserve, Curr. Opin. Neurol. 28 (6) (2015) 618–625.